Many Body Response of Benzene at Monolayer MoS_2: Van der Waals interactions and spectral broadening

Alina Umerbekova and Michele Pavanello*

Department of Chemistry, Rutgers University, Newark, NJ 07102, USA

(Dated: January 20, 2020)

Abstract

Models of surface enhancement of molecular electronic response properties are challenging for two reasons: (1) molecule-surface interactions require the simultaneous solution of the molecular and the surface dynamic response (a daunting task); (2) when solving for the electronic structure of the combined molecule+surface system, it is not trivial to single out the particular physical effects responsible for enhancement. To attack this problem, in this work we apply a formally exact decomposition of the system's response function into subsystem contributions by employing subsystem DFT which grants access to dynamic polarizabilities and optical spectra. In order to access information about the interactions between the subsystems, we extend a previously developed subsystem-based adiabatic connection fluctuation-dissipation theorem of DFT to separate the additive from the nonadditive correlation energy and identify the nonadditive correlation as the van der Waals interactions. As an example, we choose benzene adsorbed on monolayer MoS_2. We isolate the contributions to the benzene's dynamic response arising from the interaction with the surface and for the first time, we evaluate the enhancements to the effective C_6 coefficients as a function of benzene-MoS_2 distance and adsorption site. We also quantify the spectral broadening of the benzene's electronic excited states due to their interaction with the surface. We find that the broadening has a similar decay law with the molecule-surface distance as the leading van der Waals interactions (i.e., R^{-6}) and that the surface enhancement of dispersion interactions between benzene molecules is less than 5%, but still large enough (0.5 kcal/mol) to likely play a role in the prediction of interface morphologies.

* m.pavanello@rutgers.edu

I. INTRODUCTION AND BACKGROUND

The development of accurate models of materials' interfaces is a priority for materials science and engineering [1, 2]. Interfaces are key regions in energy materials such as photovoltaics [3] and photocatalysts [4] as well as in such technological applications as field-effect transistors [5]. Models must be accurate, in the sense that they need to at least reproduce the most basic of properties involved in the function of the material. These vary depending on the applications [6, 7], however such properties as the contact angle in a surface-water interface [8] thermal transport in the material [9], or the optical response [10] are among the ones widely sought after. An accurate model enables rational design of materials, which is why the model should not rely too heavily on empirical data otherwise its ability to sample outside the particular chemical space, spanned by the empirical training data, can be affected. Thus, *ab initio* methods are important tools to model materials, including their interfaces.

One important task is to test the limits of applicability of current models as well as propose new multi-scale modeling schemes that can better represent the materials under study, particularly regarding the description of materials' interfaces. In recent years, several models of 2D materials, such as metal dichalcogenides, have surfaced due to their controllable thickness and surface properties, as well as the rich array of physical and chemical properties that becomes accessible when they are interfaced with other materials [6–8]. However, these efforts are still in their infancy and the accurate and predictive model of these materials' interfaces is still largely an unsolved problem.

Thus, the particular focus of this work is to model the interface between an organic molecular system, benzene, and monolayer MoS_2. We seek to characterize how the molecular energy levels and electronic properties are affected and enhanced by the monolayer surface. For example, the fact that finite molecular states interact with an extended system gives rise to their broadening, which in turn results in the broadening of all electronic molecular observables, including the charge density. Because broadening the charge density is responsible for van der Waals interactions, such broadening might be included as a defining descriptor for molecular force fields at interfaces.

Surface enhancement is an important physical effect, which aside from the giant effects on some spectroscopies [11], it affects molecular properties such as polarizabilities as well

as other important quantities needed in the development of force fields [12, 13]. A question arises: should surface enhancement effects be accounted for when developing force fields? Similar questions have prompted the development of many-body dispersion methods [13], which aim at describing the van der Waals interactions between systems foregoing the common coarse graining of the C_6 coefficients into static, additive pair-wise contributions. Generally, the answer is that describing the nonadditive nature of van der Waals interactions is important [14]. In this work, we dive into the details of what the nonadditivity of the van der Waals interactions entail, what is its origin and its effect for the benzene-MoS_2 system considered.

All simulations presented in this work are carried out with subsystem Density Functional Theory (sDFT) [15–17]. sDFT implies that the density of the supersystem is subsystem additive,

$$\rho(\mathbf{r}) = \sum_{I}^{N_S} \rho_I(\mathbf{r}), \tag{1}$$

where N_S is the number of subsystems considered. The above equation is solved by variationally minimizing the energy functional which leads to the following coupled subsystem KS equations

$$\left[\frac{-\nabla^2}{2} + v^I_{\mathrm{KS}}(\mathbf{r}) + v^I_{\mathrm{emb}}(\mathbf{r})\right] \phi^I_i(\mathbf{r}) = \epsilon^I_i \phi^I_i(\mathbf{r}). \tag{2}$$

The embedding potential, $v^I_{\mathrm{emb}}(\mathbf{r})$, encodes all the needed interactions between I and the other subsystems. Specifically,

$$\begin{aligned} v^I_{\mathrm{emb}}(\mathbf{r}) = {} & v^I_{\mathrm{H}}[\rho](\mathbf{r}) - v^I_{\mathrm{H}}[\rho_I](\mathbf{r}) + v^I_{\mathrm{xc}}[\rho](\mathbf{r}) - v^I_{\mathrm{xc}}[\rho_I](\mathbf{r}) \\ & + v^I_{\mathrm{T_s}}[\rho](\mathbf{r}) - v^I_{\mathrm{T_s}}[\rho_I](\mathbf{r}) + \sum_{J \neq I} v^J_{\mathrm{ext}}(\mathbf{r}). \end{aligned} \tag{3}$$

In particular, an important term is the nonadditive noninteracting kinetic energy potential, $v^I_{\mathrm{T_s}}[\rho](\mathbf{r}) - v^I_{\mathrm{T_s}}[\rho_I](\mathbf{r})$. This term distinguishes sDFT from all other fragment-based electronic structure methods, and needs to be approximated and in this work we choose a GGA noninteracting kinetic energy functional [18].

The embedded Quantum ESPRESSO (eQE) software [19] developed by us, implements sDFT and the coupled equations Eq. (2). It achieves almost perfect parallel scaling and has provided a quantitative model at a much reduced computational cost compared to KS-DFT of the supersystem both for ground state dynamics simulations [20–23] as well as simulations of excited states dynamics [24–27]. To access excited states, we make use of the real-time

subsystem time-dependent DFT (TDDFT) implementation in eQE [25, 26], which solves the time-dependent Schrödinger equation within the adiabatic approximation,

$$\left[\frac{-\nabla^2}{2} + v^I_{\mathrm{KS}}(\mathbf{r},t) + v^I_{\mathrm{emb}}(\mathbf{r},t)\right]\phi^I_i(\mathbf{r},t) = i\frac{\partial\phi^I_i(\mathbf{r},t)}{\partial t}. \tag{4}$$

In this work, we close in on the response of a benzene molecule adsorbed on the surface of monolayer MoS_2. We inspect its response in several domains: (1) in the imaginary frequency domain, we quantify the degree of surface enhancement of the benzene's C_6 coefficients; (2) in the real frequency domain, we inspect the decay with respect to the molecule-surface separation of the spectral broadening (inverse lifetime) of the molecular electronic states and determine that it should follow a similar power law as the decay of the C_6 surface enhancement. We also inspect the molecular spectrum and its contribution arising from the interactions with the nearby surface. Not only do we analyze the distance dependence of these quantities, but we also inspect their dependence on the adsorption site by considering the top, hollow and bridge sites.

The paper is organized as follows. We first provide the reader with a complete theoretical background on the many-body expansion of the response functions involved and their relationship with van der Waals forces *via* the fluctuation-dissipation theorem of DFT [28–31]. We introduce a dual adiabatic connection [32–34], first connecting isolated systems to statically embedded ones (uncoupled), and then from static embedding (uncoupled) to fully interacting subsystems (coupled). This allows us to dissect the local, subsystem additive contribution to the exchange-correlation energy from the nonadditive contributions which are at the core of surface enhancement effects.

II. THEORETICAL BACKGROUND

A. Spectral broadening and observable fluctuations

A key motif in this paper is the connection between broadening (fluctuation) of molecular operators resulting from the interaction of the molecule with the surface and its effect on the molecule's properties. Spectral broadening is characterized by an imaginary energy component, Γ, in the definition of the molecular Green's function

$$G_m(E) = \left[\hat{H}_m - E + i\frac{\Gamma(E)}{2}\right]^{-1}, \tag{5}$$

which causes the molecular spectral lines to appear broad, but also has the effect of broadening other observables, such as the charge density. The charge density operator, $\hat{\rho}(\mathbf{r})$, intrinsically fluctuates around its average. A consequence of this is that the pair density becomes [28, 29]

$$\langle\Psi_0|\hat{\rho}(\mathbf{r})\hat{\rho}(\mathbf{r}')|\Psi_0\rangle = \rho(\mathbf{r})\rho(\mathbf{r}') - \frac{1}{2\pi}\int_{-\infty}^{\infty} \mathrm{Im}\left[\chi_m(\mathbf{r},\mathbf{r}',\omega)\right] d\omega, \tag{6}$$

where χ_m is the linear response function of the molecular system.

In an effort to simplify the computational cost and to reach a better understanding of how the molecular components of a system interact with each other, our group [25, 26, 30, 35] as well as many others [36–51] have looked into ways to represent properties (including response functions, polarizabilities, and other properties) of the total system as functions of subsystem quantities.

When subsystems become spatially close, the response function of the total supersystem formally follows the following expansion [35],

$$\chi = \sum_{I}^{N_S} \chi_I^c, \tag{7}$$

where

$$\chi_I^c = \chi_I^u + \sum_{I\neq J} \chi_I^u K_{IJ} \chi_J^c. \tag{8}$$

In the above, the superscript c/u stand for coupled and uncoupled, respectively, and indicate whether a subsystem is allowed/not allowed to exchange energy with other subsystems.

The uncoupled response function depends on the Kohn-Sham response function, χ_I^0, by the usual Dyson equation

$$\chi_I^u = \chi_I^0 + \chi_I^0 K_{II} \chi_I^u. \tag{9}$$

The above equations are general [36, 52, 53] because they are applicable to several density and density matrix embedding theories [54, 55]. However, when the particular case of subsystem DFT is invoked, the kernel matrix is simply defined as the functional derivative of the embedding potential of subsystem I with respect to density variations in subsystem J, $K_{IJ} = \frac{\delta v_{\mathrm{emb}}^I}{\delta \rho_J}$. This leads to the following form of the kernel,

$$K_{IJ}(\mathbf{r},\mathbf{r}',\omega) = \frac{1}{|\mathbf{r}-\mathbf{r}'|} + f_{\mathrm{xc}}[\rho](\mathbf{r},\mathbf{r}',\omega) + f_{\mathrm{T}}[\rho](\mathbf{r},\mathbf{r}',\omega) - f_{\mathrm{T}}[\rho_I](\mathbf{r},\mathbf{r}',\omega)\delta_{IJ}, \tag{10}$$

where $f_{\mathrm{xc/T}}$ is the second functional derivative of the exchange-correlation / noninteracting kinetic energy functional, and we explicitly indicate the dependence of the kernels on the total electron density given by Eq. (1) .

It is possible to exploit a many-body expansion of Eq. (8), dropping some heavy notation,

$$\chi_I^c = \underbrace{\chi_I^u}_{\text{One}} + \underbrace{\sum_{I\neq J} \chi_I^u K_{IJ} \chi_J^u}_{\text{Two}} + \underbrace{\sum_{I\neq J\neq K} \chi_I^u K_{IJ} \chi_J^u K_{JK} \chi_K^u}_{\text{Three}} + \text{Four-body} + \dots \tag{11}$$

which is useful for developing approximate methods and for understanding dynamical processes in terms of interactions between the subsystems [26, 27, 31].

B. The electron-electron interaction, V_{ee}, and the adiabatic connection formalism

Going back to the fluctuations of the pair density from Eq. (6), it is straightforward to derive the following form of the electron-electron interaction

$$\begin{aligned} V_{ee} =& \frac{1}{2}\int \mathrm{d}\mathbf{r}\mathrm{d}\mathbf{r}' \frac{\langle \Psi_0 \left|\hat{\rho}(\mathbf{r})\hat{\rho}(\mathbf{r}')\right| \Psi_0\rangle}{|\mathbf{r}-\mathbf{r}'|} \\ =& E_H[\rho] - \frac{1}{4\pi}\sum_I^{N_S} \int \mathrm{d}\mathbf{r}\mathrm{d}\mathbf{r}' \frac{\int_{-\infty}^{\infty} \mathrm{d}\omega \mathrm{Im}\left[\chi_I^u(\mathbf{r},\mathbf{r}',\omega)\right]}{|\mathbf{r}-\mathbf{r}'|} + \\ & - \frac{1}{4\pi}\sum_{I\neq J} \int \mathrm{d}\mathbf{r}\mathrm{d}\mathbf{r}' \frac{\int_{-\infty}^{\infty} \mathrm{d}\omega \mathrm{Im}\left[\int \mathrm{d}\mathbf{r}''\mathrm{d}\mathbf{r}''' \chi_I^u(\mathbf{r},\mathbf{r}'',\omega) K_{IJ}(\mathbf{r}'',\mathbf{r}''',\omega)\chi_J^c(\mathbf{r}''',\mathbf{r}',\omega)\right]}{|\mathbf{r}-\mathbf{r}'|}. \end{aligned} \tag{12}$$

Even though from the formalism so far considered, we could compute the expectation value of the electron-electron interaction, V_{ee}, we note that this is not the full value of the Hartree-exchange-correlation energy. The adiabatic connection formalism [32–34] was developed to aid this issue while still only relying on quantities at hand (i.e., without invoking the need to compute expectation values of other, one-electron operators such as the kinetic energy).

According to the adiabatic connection, the full Hartree-exchange-correlation energy is given by

$$E_H[\rho] + E_{xc}[\rho] = \int_0^1 \mathrm{d}\lambda \frac{\mathrm{d}V_{ee}[\rho](\lambda)}{\mathrm{d}\lambda} \tag{13}$$

where $V_{ee}(\lambda)$ is the electron-electron interaction of a fictitious system with the following properties:

(a) The electron-electron interaction is multiplied (scaled) by the value of λ.

(b) The electron density function is kept constant for any value of λ by changing the external potential (or the effective external potential of the KS system).

The above conditions imply working with a scaled interaction, including the inter-subsystem interaction in Eq.(10), which for $I \neq J$ becomes,

$$K_{IJ}^{\lambda}(\mathbf{r},\mathbf{r}',\omega) = \frac{\lambda}{|\mathbf{r}-\mathbf{r}'|} + f_{\mathrm{xc}}^{\lambda}[\rho](\mathbf{r},\mathbf{r}',\omega) + f_{\mathrm{T}}^{\lambda}[\rho](\mathbf{r},\mathbf{r}',\omega), \tag{14}$$

The scaled kernels must be evaluated with the scaled density according to previously derived prescriptions [29, 56]. The above also implies that the scaled Hartree energy $E_H(\lambda) = \lambda E_H(1)$, and therefore the integral in Eq.(13) has no effect on it.

C. The adiabatic connection for interacting subsystems

In a subsystem formulation, the adiabatic connection integral can be split into two parts, one that carries out only the *inter-subsystem* adiabatic connection and one for the *intra-subsystem* part. We use two distinct coupling strength integrations, one over λ and one over λ'. Thus, the kernel can be represented by a square matrix of leading size the number of subsystems, N_S, and as a sum of a diagonal part and a purely off-diagonal part.

$$\mathbf{K}^{\lambda,\lambda'} = \mathbf{K}_{\mathrm{intra}}^{\lambda} + \mathbf{K}_{\mathrm{inter}}^{\lambda'} \tag{15}$$

where,

$$\mathbf{K}_{\mathrm{intra}}^{\lambda} \equiv \begin{bmatrix} K_{11}^{\lambda} & 0 & \cdots & 0 \\ 0 & K_{22}^{\lambda} & \cdots & 0 \\ 0 & 0 & \ddots & \vdots \\ 0 & 0 & \ldots & K_{N_S N_S}^{\lambda} \end{bmatrix} \tag{16}$$

and

$$\mathbf{K}_{\mathrm{inter}}^{\lambda'} \equiv \begin{bmatrix} 0 & K_{12}^{\lambda'} & \cdots & K_{1N_S}^{\lambda'} \\ K_{21}^{\lambda'} & 0 & \cdots & K_{2N_S}^{\lambda'} \\ K_{31}^{\lambda'} & K_{32}^{\lambda'} & \ddots & \vdots \\ K_{N_S 1}^{\lambda'} & K_{N_S 2}^{\lambda'} & \ldots & 0 \end{bmatrix} \tag{17}$$

The corresponding terms making up the electron-electron interaction are then intra- and inter-subsystem. The intra-subsystem (additive) exchange-correlation energy for a subsystem becomes,

$$E_{xc}^{I} = -\frac{1}{4\pi}\int \mathrm{d}\mathbf{r}\mathrm{d}\mathbf{r}' \frac{\int_0^1 \mathrm{d}\lambda \int_{-\infty}^{+\infty} \mathrm{d}\omega \ \mathrm{Im}\left[\chi_I^u(\mathbf{r},\mathbf{r}',\omega;\lambda)\right]}{|\mathbf{r}-\mathbf{r}'|}, \tag{18}$$

where the additional dependence of the subsystem response function on the adiabatic connection coupling strength is explicitly indicated.

The inter-subsystem (nonadditive) contributions become

$$E_{xc}^{IJ} = E_{xc}^{JI} = -\frac{1}{4\pi}\int \mathrm{d}\mathbf{r}\mathrm{d}\mathbf{r}' \frac{\int_0^1 \mathrm{d}\lambda' \int_{-\infty}^{\infty} \mathrm{d}\omega \mathrm{Im}\left[\int \mathrm{d}\mathbf{r}''\mathrm{d}\mathbf{r}'''\chi_I^u(\mathbf{r},\mathbf{r}'',\omega)K_{IJ}^{\lambda'}(\mathbf{r}'',\mathbf{r}''',\omega)\chi_J^c(\mathbf{r}''',\mathbf{r}',\omega;\lambda')\right]}{|\mathbf{r}-\mathbf{r}'|}. \tag{19}$$

It is important to point out that the two adiabatic-connection integrations are not commutative. That is, the λ integration should be carried out first to obtain locally (uncoupled) interacting subsystem response functions. In a second step, the integration over λ' yields the remaining inter-subsystem correlation energy. Integrating in the reverse order, should still yield the correct final result, however, the additive and nonadditive contributions would not have a clear physical meaning.

In our previous works on nonadditive exchange-correlation [30, 31], we employed the many-body perturbative expansion of χ_J^c in a way similar to Eq.(11) to only include one and two-body terms. We expect that a two-body truncation will be sufficient for molecular dimers. However, in the condensed phase the two-body truncation will not be a good approximation. This is reminiscent of the so-called many-body dispersion [43, 44] which has been shown to be an extremely important effect in condensed phases [44] and particularly in large nanostructures [57].

In practical simulations, such as when force fields are employed, van der Waals interactions are encoded with the so-called C_6 coefficients. These can be derived from Eq.(19) by the following approximations

- The exchange-correlation and kinetic energy kernels are neglected. Namely, $K_{IJ}^{\lambda}(\mathbf{r},\mathbf{r}',\omega) \simeq \frac{\lambda}{|\mathbf{r}-\mathbf{r}'|}$. This goes by the name "RPA approximation".

- The density-density response functions of the subsystems are fairly well spatially separated and thus can be approximated as fluctuating dipoles. This implies the use of

frequency dependent dipole polarizabilities, instead, defined as follows:

$$\alpha^{c/u}_{I_{(ij)}}(\omega) = \int \mathrm{d}\mathbf{r}\mathrm{d}\mathbf{r}'\mathbf{r}_i\chi^{c/u}_I(\mathbf{r},\mathbf{r}',\omega)\mathbf{r}'_j, \tag{20}$$

where $\mathbf{r}_i$ can be any of the three Cartesian directions (e.g., x, y or z).

As a result of the above approximation, the Coulomb kernel must be changed to the interaction between two dipoles, which takes the form

$$\frac{1}{|\mathbf{r}-\mathbf{r}'|} \rightarrow \mathbf{T}(\mathbf{r},\mathbf{r}') = \frac{\partial}{\partial\mathbf{r}_i}\frac{\partial}{\partial\mathbf{r}'_j}\frac{1}{|\mathbf{r}-\mathbf{r}'|}, \tag{21}$$

which asymptotically goes like $\frac{1}{R^3_{IJ}}$, with R_{IJ} being the distance between the centers of charge of subsystems I and J. And thus, Eq.(19) becomes

$$E^{IJ}_{xc} = -\frac{1}{4\pi}\int_0^1 \mathrm{d}\lambda' \int_{-\infty}^{\infty} \mathrm{d}\omega \sum_{ijkl} \alpha^u_{I_{(ij)}}(i\omega)T_{jk}\lambda'\alpha^c_{J_{(kl)}}(i\omega;\lambda')T_{li} \tag{22}$$

The integral over λ' yields a factor of $\frac{1}{2}$. However, because $E^{IJ}_{xc} = E^{JI}_{xc}$ and both terms need to be accounted for (Eq.(12) removes this double counting problem) a factor of 2 arises. Thus, in the full-potential approximation [58, 59], and changing the integration to only sum over the positive frequency axis,

$$E^{IJ}_{xc} + E^{JI}_{xc} = E^{int}_{xc} = -\frac{1}{2\pi}\int_0^{\infty} \mathrm{d}\omega \sum_{ijkl} \alpha^u_{I_{(ij)}}(i\omega)T_{jk}\alpha^c_{J_{(kl)}}(i\omega)T_{li}, \tag{23}$$

Which leads to the following definitions of the so-called C_6 coefficients:

$$C^u_6 = \frac{3}{\pi}\int \mathrm{d}\omega \alpha^u_{I_{(ij)}}(i\omega)\alpha^u_{J_{(kl)}}(i\omega), \tag{24}$$

$$C^c_6 = \frac{3}{\pi}\int \mathrm{d}\omega \alpha^c_{I_{(ij)}}(i\omega)\alpha^u_{J_{(kl)}}(i\omega). \tag{25}$$

Their difference, $C^c_6 - C^u_6$, is a measure of the many-body effects of the environment on the interaction between subsystem I and J.

III. INTERACTION OF MOLECULAR SUBSYSTEMS NEARBY A SURFACE

When molecular systems are in the proximity of extended systems the so-called nonadditivity of the van der Waals interactions is non-negligible [14]. In this work, we aim at determining how molecular van der Waals interactions are affected by the presence of a

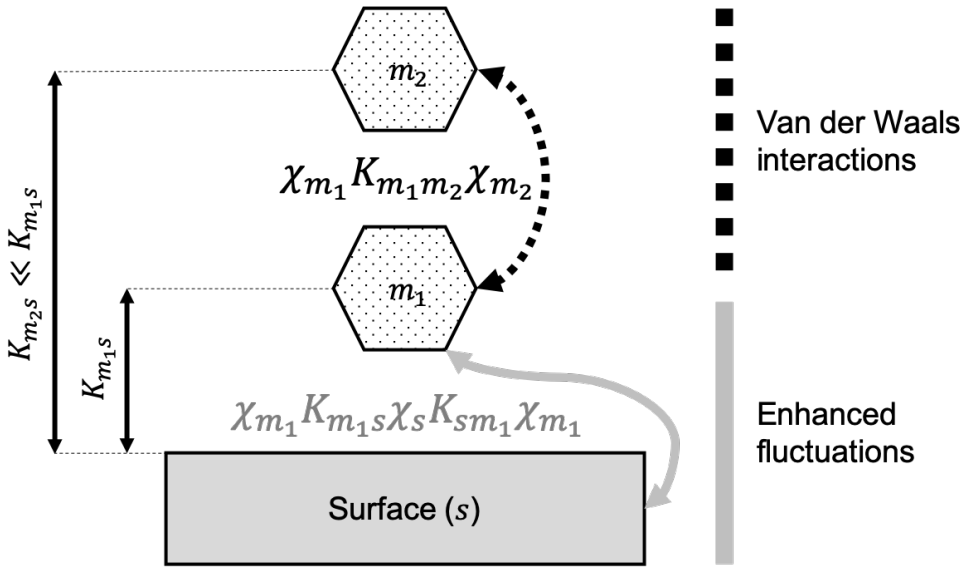

FIG. 1: The van der Waals interaction between two benzene molecules m_1 and m_2 is indicated by the dashed back arrow and is mediated by the density fluctuations originating from coupling of the molecular response functions, dropping the u and c superscripts: $\chi_{m_1} K_{m_1 m_2} \chi_{m_2}$. When m_1 is nearby an extended surface, the interactions between m_1 and m_2 depend on the distance between m_1 and the surface because the density fluctuations of m_1 are augmented by the interaction with the adjacent surface. This is indicated by the grey arrow and the term $\chi_{m_1} K_{m_1 s} \chi_s K_{s m_1} \chi_{m_1}$. In this sense, van der Waals interactions are not additive.

nearby extended surface. In other words, this translates to wondering the question: Will there be a dependence of molecular C_6 coefficients with respect to the distance between the molecular systems and a nearby surface? Figure 1 provides a visual for the effect we seek to shed light on in this work.

In order to inspect this effect we need to develop a slight variant of the response formalism presented so far. Specifically, we need to extend the formalism to a situation where we allow the application of external perturbations only to one subsystem, say the molecule or m, while keeping the surface, s, away from the applied external perturbation. The formalism simplifies to (note the subscripts m and s indicating the molecule and surface subsystems,

respectively),

$$\chi^c_m = \chi^u_m + \chi^u_m K_{ms} \chi^u_s K_{sm} \chi^c_m, \tag{26}$$

$$\chi^c_s = \chi^u_s K_{sm} \chi^c_m. \tag{27}$$

The absence of the one body term in Eq. (27) is due to the assumption that we are only interested in the molecular subsystem. Thus, all external perturbing fields are applied to only the molecular subsystem while the surface subsystem, responding according to χ_s, is perturbed *via* the Coulomb interactions with the density fluctuations of m. That is, the externally applied potential on the surface, δv^s_{appl}, is the Coulomb interactions due to the density response of the molecular system, $\delta v^s_{\text{appl}} = K_{sm} \chi^{u/c}_m$.

In determining the exchange-correlation energy of interaction between molecules when they are nearby the surface, the surface has the effect of modifying and enhancing the molecule's density fluctuations. Specifically, the response function integrand in Eq. (19) when one molecule m_1 interacts with another m_2, while m_1 is nearby a surface,

$$E^{m_2 m_1}_{xc} = -\frac{1}{4\pi} \int \mathrm{d}\mathbf{r}\mathrm{d}\mathbf{r}' \frac{\int_0^1 \mathrm{d}\lambda' \int_{-\infty}^{\infty} \mathrm{d}\omega \mathrm{Im} \left[\int \mathrm{d}\mathbf{r}''\mathrm{d}\mathbf{r}''' \chi^u_{m_2}(\mathbf{r}, \mathbf{r}'', \omega) K^{\lambda'}_{m_2 m_1}(\mathbf{r}'', \mathbf{r}''', \omega) \chi^c_{m_1}(\mathbf{r}''', \mathbf{r}', \omega; \lambda') \right]}{|\mathbf{r} - \mathbf{r}'|}. \tag{28}$$

However, due to Eq. (26), and dropping the heavy notation substituting it with a generalized trace operator over the frequency, ω, and coupling strength, λ,

$$E^{m_2 m_1}_{xc} = \int \mathrm{d}\mathbf{r}\mathrm{d}\mathbf{r}' \frac{\mathrm{Tr}_{(\omega,\lambda')} \left\{ \mathrm{Im} \left[\chi^u_{m_2} K^{\lambda'}_{m_2 m_1} \chi^u_{m_1} + \chi^u_{m_2} K^{\lambda'}_{m_2 m_1} \chi^u_{m_1} K^{\lambda'}_{m_1 s} \chi^u_s K^{\lambda'}_{s m_1} \chi^c_{m_1}(\lambda') \right] \right\}}{|\mathbf{r} - \mathbf{r}'|}. \tag{29}$$

The above equation clearly shows a first term, dependent on $\chi^u_{m_2} K_{m_2 m_1} \chi^u_{m_1}$, which would be present even if the surface was ignored. And a term, dependent on $\chi^u_{m_2} K_{m_2 m_1} \chi^u_{m_1} K_{m_1 s} \chi^u_s K_{s m_1} \chi^c_{m_1}$, which results exclusively from the presence of the surface. The latter can be thought of as a surface enhancement effect. We will image the surface effects by computing optical spectra and C_6 coefficients according to Eq. (24–25).

IV. COMPUTATIONAL DETAILS

To best highlight the surface enhancements of the van der Waals interactions between molecular systems nearby an extended surface, we consider a benzene molecule adsorbed on

the surface of monolayer molybdenum sulfide. We then computationally evaluate the optical spectrum (including characterization of the spectral broadening of the first molecular excitation) and the effective molecular C_6 coefficient progressing from an isolated molecule, to an embedded but dynamically uncoupled molecule (i.e., the C_6^u from Eq. (24)) to a molecule fully coupled to the surface (i.e., the C_6^c from Eq. (25)). This will shed light on the size of the surface enhancement effect of the effective C_6 coefficients, the decay law as a function of the distance to the surface, as well as its relationship with the spectral broadening.

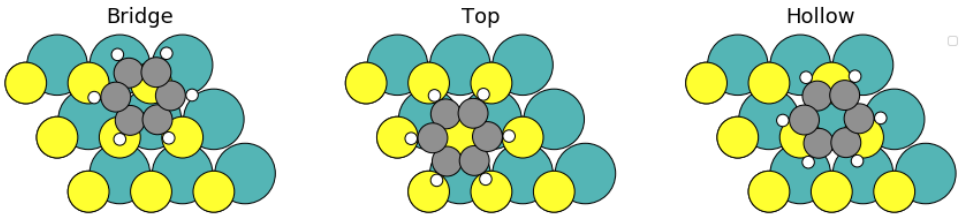

FIG. 2: A top-view depiction of the three adsorption sites considered in this work.

All calculations are carried out with a development version of eQE [19] and the associated subsystem real-time TDDFT code [25]. We employ ultrasoft pseudopotentials from the GBRV library [60], and a plane wave cut off of 50 Ry for the wavefunctions and 500Ry for the charge density. This is appropriate given that we employ ultrasoft pseudopotentials.

The real-time TDDFT simulations were carried out with a Crank-Nicolson propagator with a single predictor-corrector step, a time step of 2 as, and a total of 20,000 steps. We traced out the time-dependent subsystem density and computed the time-dependent dipole change, $\delta\mu(t) = \mu(t) - \mu(0)$ in the same direction as the applied external electric field. The field was applied with the "kick" method [61]. Once the time-dependent dipole change is obtained we proceeded to Fourier transform to frequency space for plotting optical spectra, and Laplace transform to imaginary frequency space for computing the effective C_6 coefficients.

TABLE I: Benzene's static dipole polarizability, α_{xx}, of benzene adsorbed at the hollow site of MoS_2 along the x direction for several separations, R in Å, from the surface. Polarizability values in atomic units.

R	α_{xx}^{iso}	α_{xx}^{u}	α_{xx}^{c}
3.50	93.76	96.05	99.01
3.75	93.76	95.40	97.38
4.00	93.76	95.25	96.54
4.25	93.76	95.03	95.95
4.50	93.76	95.08	95.72

V. RESULTS

We structure the results section into two subsections. The first one regards van der Waals interactions and their surface enhancement. The second one regards the effect of the surface on the optical spectrum of the adsorbed benzene molecule. Then, we compare the spectral broadening, Γ with the surface enhancement of the effective C_6 coefficient and show that they follow a similar power law for the decay as a function of the distance from the surface.

A. Polarizabily and van der Waals interactions

We start by considering the molecular static dipole polarizability, which is also affected by the presence of the surface. In Table I we list the values of α_{xx} for the benzene molecule when it is isolated, and nearby the surface as uncoupled, and coupled. Hereafter, the superscripts c and u will carry the same meaning as in the previous sections.

As described by Eq. (29), the interaction with the surface induces additional density fluctuations in adsorbed molecular systems. In Figure 3(b), we show the surface enhancement for $\alpha_m(i\omega)$ by plotting the quantities $\alpha_m^c(i\omega)$, $\alpha_m^u(i\omega)$ and $\alpha_m^{iso}(i\omega)$. From the table it is clear that the surface enhancement on the static dipole polarizability is of at most 5% for the shortest distance of $R = 3.5$Å. This seems reasonable, as the MoS_2 surface is not as polarizable as a metal surface for which larger enhancements have been reported [27].

In addition to the dipole polarizability, also the effective C_6 coefficients are affected by the presence of a nearby surface. This is the direct consequence of Eq. (29). Thus, we computed

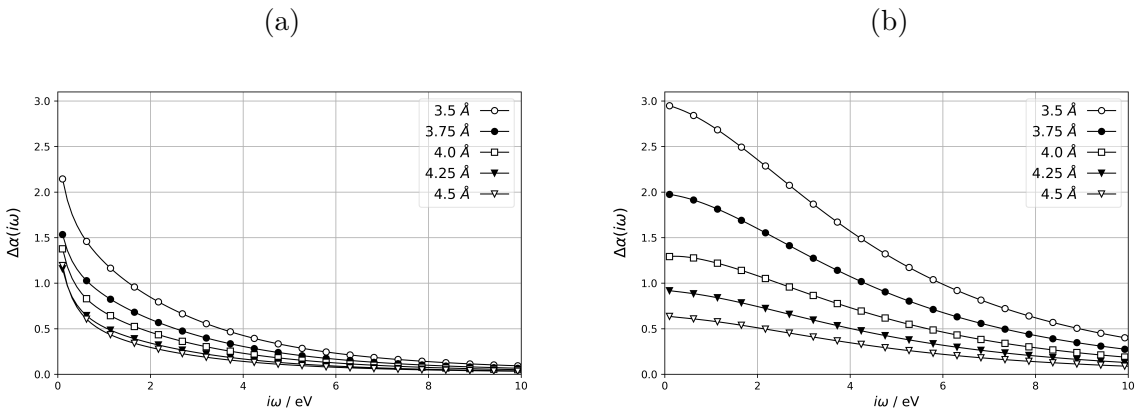

FIG. 3: Benzene's dipole polarizability as a function of imaginary frequency and for several molecule-surface separations. Inset (a): $\alpha_m^u(i\omega) - \alpha_m^{iso}(i\omega)$, the polarizability difference between a molecule nearby the MoS_2 surface that is not allowed to respond dynamically (i.e., molecule and surface cannot exchange energy) and an isolated molecule. Inset (b): $\alpha_m^c(i\omega) - \alpha_m^u(i\omega)$, displaying the enhancement when the molecule and the surface are fully coupled and can exchange energy.

TABLE II: The x contribution to the effective C_6 coefficient of benzene adsorbed at the hollow site of MoS_2 and for several separations, R in Å, from the surface. C_6 values are given in atomic units. The superscripts *iso*, *u* and *c* bear the same meaning as in Table I.

R	C_6^{iso}	C_6^u	C_6^c
3.50	2734	2765	2809
3.75	2734	2756	2786
4.00	2734	2751	2771
4.25	2734	2747	2761
4.50	2734	2746	2755

the effective C_6 coefficients for the isolated, uncoupled and coupled cases. The results are listed in Table II.

In order to compare our results to the literature, we have computed isotropic polarizability and isotropic C_6 coefficient for an isolated benzene molecule. Our values, $\alpha^{iso} = 76.5$ a.u. and $C_6^{iso} = 1961$ a.u., agree well with reference values, $\alpha^{iso} = 71.3$ a.u. and $C_6^{iso} = 1723$ a.u.[62]. The result for C_6^{iso} coefficient compares very closely to the value 1956.8 a.u. [63]

TABLE III: Expected total dispersion energy (E_{disp}) between two benzene molecules stacked on top of a MoS_2 surface. We report also the surface enhancement as a function of distance and brake it down into isolated-to-uncoupled (ΔE_{disp}^{iso-u}) and uncoupled-to-coupled (ΔE_{disp}^{u-c}) contributions. %SE stands for surface enhancement. Energy values in kcal/mol.

R	E_{disp}	ΔE_{disp}^{iso-u}	ΔE_{disp}^{u-c}	%SE
3.50	21.055	0.236	0.327	2.7
3.75	13.804	0.111	0.147	1.9
4.00	9.323	0.059	0.067	1.4
4.25	6.456	0.031	0.032	1.0
4.50	4.572	0.020	0.016	0.8

TABLE IV: Comparison between the C_6 coefficients computed at different benzene adsorption sites on MoS_2 for a benzene-surface separation of $R = 3.5$Å.

	C_6^{hol}	C_6^{bri}	C_6^{top}
isolated	2734	2734	2734
uncoupled	2765	2763	2765
coupled	2809	2806	2808

computed at the Hartree-Fock level.

In Table III we report the surface effects on the dispersion interactions between two benzene molecules affected by the presence of the monolayer MoS_2 surface. The total surface enhancement of the dispersion interaction is about 0.5 kcal/mol or about 3% at 3.5 Å separation.

When comparing the C_6 coefficients for the three sites (hollow, bridge and top) their values are largely similar, see Table IV. This shows that the coupling with the surface is on average similar for the three sites. Due to their dependency on the integral over imaginary frequency of the dipole response function, the C_6 coefficients reflect a coupling to the surface that is somewhat averaged over all frequencies.

B. Optical spectra

In Figure 4 we report the comparison between the optical spectrum of uncoupled benzene at $R = 3.5$Å with the experimentally determined optical spectrum of a sample of benzene vapor. The two spectra are in fair agreement even though our simulations are carried out with a semilocal exchange-correlation functional (e.g., the predicted band gap is smaller than the reference band gap). The quality of the experiment-theory comparison in the

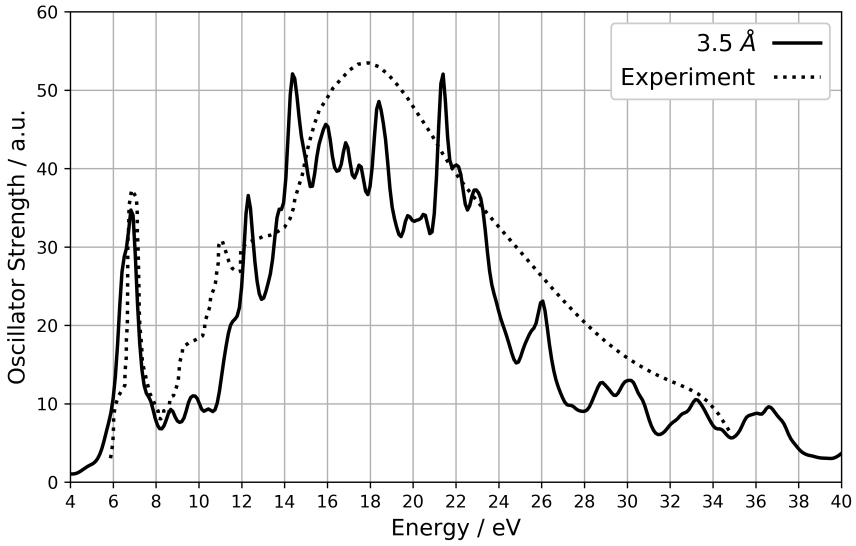

FIG. 4: Comparison of the computed and experimental spectra of benzene. The computed spectrum is for the uncoupled benzene adsorbed at the hollow site of MoS_2 at a molecule-surface separation of $R = 3.5$Å. The experimental spectrum is for a sample of gas phase benzene [64].

broad energy window $4 < \omega < 40$ constitute the underlying reasons for the good agreement between our calculations and other simulations on the frequency dependent polarizabilities and C_6 coefficients.

The effect of the interaction with the surface can be singled out by visualizing the coupled-uncoupled deviation in the optical spectrum of benzene, see Figure 5. Such a deviation is due almost entirely to three-body terms in the expansion Eq.(11), and follows a trend that we witnessed before [27] when we considered the optical spectra of benzene on MoS_2 in a standing configuration. The three-body terms are quite interesting. They feature a

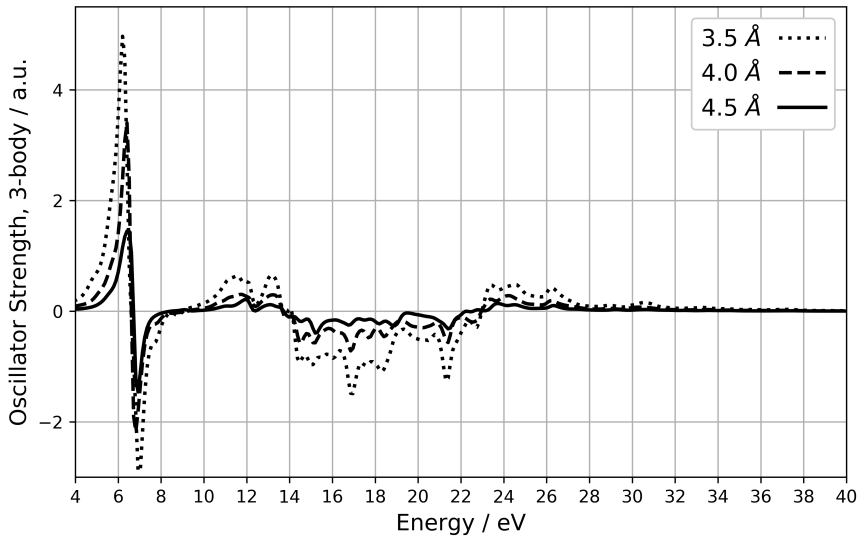

FIG. 5: Oscillator strength contribution from three-body terms (and higher order) in the many body expansion of the response function, Eq.(11), for several molecule-surface separations.

derivative-like behavior which is needed to shift the peak to the lower energies (i.e., red shift when molecules are adsorbed on surfaces is commonly recorded) and at the same time they feature a characteristic peak broadening. This is at the heart of the surface enhancements effects. Such a characteristic broadening is a signature of the extent to which molecular and surface quantum states couple.

The optical spectra are in principle dependent on the adsorption configuration. We analyze this in Figure 6, where we compare the deviation from the average spectrum of the spectra obtained from benzene adsorbed at the hollow, top and bridge sites. We break down the comparison into isolated to uncoupled and uncoupled to coupled. We notice that the isolated to uncoupled offers the largest deviation. This is understandable because the coupling of the molecular states with the bands of the semiconductor (giving rise to the uncoupled-to-coupled deviation) should only be weakly dependent on translations, and instead be strongly dependent on the molecule-surface distance. As expected, the top and hollow sites yield mirrored deviations in both cases.

(a) (b)

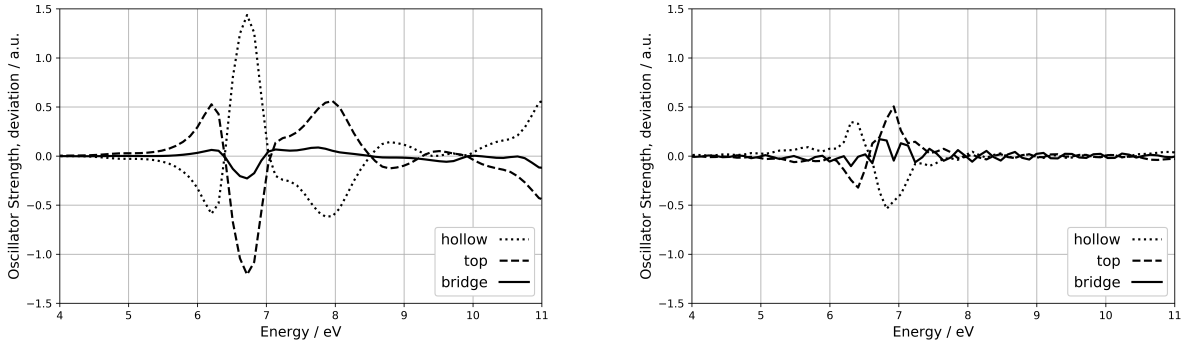

FIG. 6: Comparison of the isolated-uncoupled [inset (a)], and uncoupled-coupled [inset(b)] spectra of benzene adsorbed at the hollow, top and bridge sites of MoS_2 at a molecule-surface separation of $R = 3.5$Å. Here we plot the deviation from the average of the three spectra.

C. Comparison of spectral broadening and surface enhancement of C_6 coefficients

The spectral broadening introduced in Eq.(5) can be defined in terms of the subsystem response functions [27]. Eq.(26) can be recast in the following form,

$$\chi_m^c = \chi_m^u + \chi_m^u K_{\rm open} \chi_m^c, \tag{30}$$

where

$$K_{\rm open} = K_{ms} \chi_s^u K_{sm} \tag{31}$$

implying that when a subsystem is open to exchanging energy with the surrounding, the TDDFT kernel, K, should be augmented, $K \to K + K_{\rm open}$ [26].

Eq.(5) indicates that the spectral broadening is related to the imaginary part of $K_{\rm open}$. Thus, we expect the distance dependence of the spectral broadening to match the distance dependence of the C_6 surface enhancement. Computation of the first peak line shape is complicated by splitting of the peak for the close molecule-surface separations. We overcome this difficulty by computing broadenings of both the peak and the shoulder, and summing them together.

Figure 7 displays in log scale the decay with distance of the spectral broadening and the surface enhancement of the C_6 coefficient for the benzene adsorbed on the hollow site.

The deviation at 4.0 Å for the broadening value arises due to peak and shoulder merge being incomplete at that distance. From the figure we derive a power decay law for the

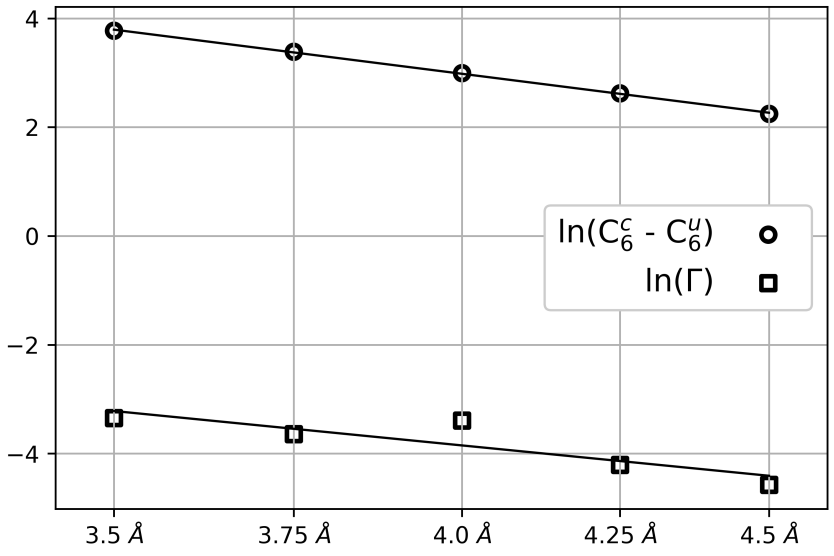

FIG. 7: The molecule-surface distance decay of the surface enhancement of the effective C_6 coefficient compared to the decay of the surface-induced spectral broadening. Note the log scale for both x and y axes.

broadening of $n_\Gamma = 4.8 \pm 0.6$ for the Lorentzian-profile. The power decay law for the surface enhancement of the C_6 coefficients is $n_{C_6} = 6.1$ with a negligible standard deviation. These are in fair agreement.

The broadening values for all configurations considered are collected in the supplementary material jupyter notebooks [65] and range from 10 to 35 meV for the hollow site adsorption. This is less than (however, in the same order of magnitude) the broadening of atomic levels at metal surfaces [66, 67]. The top and hollow sites show similar values, unlike the bridge site which displays the largest broadening value of 117 meV. This indicates a stronger molecule-surface interaction at the particular frequency of the excitation energy of benzene, which could be explained by a higher density of states at the bridge site. Such effect was also observed in the DFT calculations for an AFM tip on graphene/Ni substrate [68].

VI. CONCLUSIONS

In this work, we outline a road map to compute such important quantities as C_6 coefficients, dipole polarizabilities and optical spectra of molecular systems embedded in complex environments. We do so by leveraging the subsystem TDDFT formalism and by means of the adiabatic-connection fluctuation-dissipation theorem of DFT. Our method is capable of isolating the molecule-environment interactions responsible for interesting dynamical behaviors, such as surface enhancement.

We showcase the method by considering a benzene molecule adsorbed on the surface of monolayer MoS_2, showing that the enhancement of the molecular properties on the monolayer is nonnegligible and should be taken into account when developing simpler and coarse grained models of molecule-surface interfaces. Even though monolayer MoS_2 is not nearly as polarizable as a metal surface, the molecular static polarizabilities showed a notable enhancement when the molecule is coupled to the surface, with the effect becoming negligible at larger distances. Dispersion interactions are enhanced by about 0.5 kcal/mol for each molecular dimer at typical van der Waals distances. Although limited in size, such an enhancement can change the predicted morphology of the interface.

In an effort to bring all surface enhancements under the same framework, we relate the surface enhancement of the C_6 coefficients to the broadening of the molecular energy levels due to the interaction with the surface. The formalism predicts an identical decay of these quantities as a function of the molecule-surface distance equal to the inverse sixth power of the distance, while the computations reveal a slight difference of (yet) unknown origin.

The natural future developments for this work will involve deriving surface-aware force field parameters that tune the dispersion and electrostatic interactions in a way that is computationally cheaper than solving the coupled system of equations, as done vdW-TS [44] and polarizable force fields [69], while still being accurate enough to capture the relevant environment and surface induced enhancements.

ACKNOWLEDGMENTS

This material is based upon work supported by the U.S. Department of Energy, Office of Basic Energy Sciences, under Award Number DE-SC0018343. The authors acknowledge

the Office of Advanced Research Computing (OARC) at Rutgers, The State University of New Jersey for providing access to the Amarel cluster and associated research computing resources that have contributed to the results reported here. URL: http://oarc.rutgers.edu

---

[1] O. Björneholm, M. H. Hansen, A. Hodgson, L.-M. Liu, D. T. Limmer, A. Michaelides, P. Pedevilla, J. Rossmeisl, H. Shen, G. Tocci, E. Tyrode, M.-M. Walz, J. Werner, and H. Bluhm, Chem. Rev. **116**, 7698 (2016).

[2] P. Schulz, D. Cahen, and A. Kahn, Chem. Rev. **119**, 3349 (2019).

[3] F. De Angelis, S. Fantacci, and R. Gebauer, J. Phys. Chem. Lett. **2**, 813 (2011).

[4] I. X. Green, W. Tang, M. Neurock, and J. T. Yates, Science **333**, 736 (2011), http://www.sciencemag.org/content/333/6043/736.full.pdf.

[5] S. Wang, S. Dhar, S. rui Wang, A. C. Ahyi, A. Franceschetti, J. R. Williams, L. C. Feldman, and S. T. Pantelides, Phys. Rev. Lett. **98** (2007), 10.1103/physrevlett.98.026101.

[6] Z. Gu, P. D. Luna, Z. Yang, and R. Zhou, Phys. Chem. Chem. Phys. **19**, 3039 (2017).

[7] M. Heiranian, Y. Wu, and N. R. Aluru, J. Chem. Phys. **147**, 104706 (2017).

[8] B. Luan and R. Zhou, Appl. Phys. Lett. **108**, 131601 (2016).

[9] V. Varshney, S. S. Patnaik, C. Muratore, A. K. Roy, A. A. Voevodin, and B. L. Farmer, Comput. Mater. Sci. **48**, 101 (2010).

[10] S. Gupta, S. N. Shirodkar, A. Kutana, and B. I. Yakobson, ACS Nano **12**, 10880 (2018).

[11] S. M. Morton and L. Jensen, J. Am. Chem. Soc. **131**, 4090 (2009).

[12] K. Szalewicz, WIREs: Comput. Mol. Sci. **2**, 254 (2011).

[13] J. Hermann, R. A. DiStasio, and A. Tkatchenko, Chem. Rev. **117**, 4714 (2017).

[14] A. Ruzsinszky, J. P. Perdew, J. Tao, G. I. Csonka, and J. M. Pitarke, Phys. Rev. Lett. **109** (2012), 10.1103/physrevlett.109.233203.

[15] A. Krishtal, D. Sinha, A. Genova, and M. Pavanello, J. Phys.: Condens. Matter **27**, 183202 (2015).

[16] T. A. Wesolowski, S. Shedge, and X. Zhou, Chem. Rev. **115**, 5891 (2015).

[17] C. R. Jacob and J. Neugebauer, WIREs: Comput. Mol. Sci. **4**, 325 (2014).

[18] S. Laricchia, E. Fabiano, L. A. Constantin, and F. Della Sala, J. Chem. Theory Comput. **7**, 2439 (2011).

[19] A. Genova, D. Ceresoli, A. Krishtal, O. Andreussi, R. DiStasio Jr., and M. Pavanello, Int. J. Quantum Chem. **117**, e25401 (2017).

[20] A. Genova and M. Pavanello, J. Phys.: Condens. Matter **27**, 495501 (2015).

[21] A. Genova, D. Ceresoli, and M. Pavanello, J. Chem. Phys. **141**, 174101 (2014).

[22] A. Genova, D. Ceresoli, and M. Pavanello, J. Chem. Phys. **144**, 234105 (2016).

[23] W. Mi, P. Ramos, J. Maranhao, and M. Pavanello, J. Phys. Chem. Lett. **10**, 7554 (2019).

[24] S. K. P., A. Genova, and M. Pavanello, J. Phys. Chem. Lett. **8**, 5077 (2017).

[25] A. Krishtal, D. Ceresoli, and M. Pavanello, J. Chem. Phys. **142**, 154116 (2015).

[26] A. Krishtal and M. Pavanello, J. Chem. Phys. **144**, 124118 (2016).

[27] A. Umerbekova, S.-F. Zhang, S. K. P., and M. Pavanello, Eur. Phys. J. B **91** (2018), 10.1140/epjb/e2018-90145-2.

[28] W. Kohn, Y. Meir, and D. E. Makarov, Phys. Rev. Lett. **80**, 4153 (1998).

[29] F. Furche and T. Van Voorhis, J. Chem. Phys. **122**, 164106 (2005).

[30] R. Kevorkyants, H. Eshuis, and M. Pavanello, J. Chem. Phys. **141**, 044127 (2014).

[31] D. Sinha and M. Pavanello, J. Chem. Phys. **143**, 084120 (2015).

[32] A. Savin, F. Colonna, and R. Pollet, Int. J. Quantum Chem. **93**, 166 (2003).

[33] K. Burke, J. Werschnik, and E. K. U. Gross, J. Chem. Phys. **123**, 062206 (2005).

[34] D. C. Langreth and J. P. Perdew, Phys. Rev. B **15**, 2884 (1977).

[35] M. Pavanello, J. Chem. Phys. **138**, 204118 (2013).

[36] J. Neugebauer, J. Chem. Phys. **126**, 134116 (2007).

[37] J. Neugebauer, J. Phys. Chem. B **112**, 2207 (2008).

[38] J. Neugebauer, Phys. Rep. **489**, 1 (2010).

[39] J. Neugebauer, in *Recent Advances in Orbital-Free Density Functional Theory*, edited by T. A. Wesolowski and Y. A. Wang (World Scientific, Singapore, 2013).

[40] J. Neugebauer, J. Chem. Phys. **131**, 084104 (2009).

[41] J. Neugebauer, ChemPhysChem **10**, 3148 (2009).

[42] J. Neugebauer, C. Curutchet, A. Munioz-Losa, and B. Mennucci, J. Chem. Theory Comput. **6**, 1843 (2010).

[43] X. Ge and D. Lu, Phys. Rev. B **96** (2017).

[44] R. A. DiStasio, V. V. Gobre, and A. Tkatchenko, J. Phys.: Condens. Matter **26**, 213202 (2014).

[45] M. J. Gillan, D. Alfe, P. J. Bygrave, C. R. Taylor, and F. R. Manby, J. Chem. Phys. **139**, 114101 (2013).

[46] L. D. Jacobson and J. M. Herbert, J. Chem. Phys. **134**, 094118 (2011).

[47] R. M. Richard and J. M. Herbert, J. Chem. Phys. **137**, 064113 (2012).

[48] J. Liu and J. M. Herbert, J. Chem. Phys. **143**, 034106 (2015).

[49] D. Pan, M. Govoni, and G. Galli, J. Chem. Phys. **149**, 051101 (2018).

[50] A. S. P. Gomes and C. R. Jacob, Annu. Rep. Prog. Chem., Sect. C: Phys. Chem. **108**, 222 (2012).

[51] S. Höfener, A. S. P. Gomes, and L. Visscher, J. Chem. Phys. **136**, 044104 (2012).

[52] M. A. Mosquera, D. Jensen, and A. Wasserman, Phys. Rev. Lett. **111**, 023001 (2013).

[53] M. E. Casida and T. A. Wesolowski, Int. J. Quantum Chem. **96**, 577 (2004).

[54] G. H. Booth and G. K.-L. Chan, Phys. Rev. B **91**, 155107 (2015).

[55] Q. Sun and G. K.-L. Chan, Acc. Chem. Res. **49**, 2705 (2016).

[56] P. Hessler, J. Park, and K. Burke, Phys. Rev. Lett. **82**, 378 (1999).

[57] A. Ambrosetti, N. Ferri, R. A. DiStasio, and A. Tkatchenko, Science **351**, 1171 (2016).

[58] D. C. Langreth, M. Dion, H. Rydberg, E. Schröder, P. Hyldgaard, and B. I. Lundqvist, Int. J. Quantum Chem. **101**, 599 (2005).

[59] J. F. Dobson and T. Gould, J. Phys.: Condens. Matter **24**, 073201 (2012).

[60] K. F. Garrity, J. W. Bennett, K. M. Rabe, and D. Vanderbilt, Computational Materials Science **81**, 446 (2014).

[61] K. Yabana and G. F. Bertsch, Phys. Rev. B **54**, 4484 (1996).

[62] V. V. Gobre and A. Tkatchenko, Nature Communications **4** (2013), 10.1038/ncomms3341.

[63] I. Adamovic and M. S. Gordon, Molecular Physics **103**, 379 (2005).

[64] E. Koch and A. Otto, Chem. Phys. Lett. **12**, 476 (1972).

[65] "See Supplementary Material Document at [URL will be inserted by publisher] for additional tables and figures.".

[66] E. V. Chulkov, A. G. Borisov, J. P. Gauyacq, D. Sánchez-Portal, V. M. Silkin, V. P. Zhukov, and P. M. Echenique, Chem. Rev. **106**, 4160 (2006).

[67] P. Nordlander and J. C. Tully, Phys. Rev. B **42**, 5564 (1990).

[68] L. Gao, Y. Ma, Y. Liu, A. Song, T. Ma, Y. Hu, Y. Su, and L. Qiao, The Journal of Physical Chemistry C **121**, 21397 (2017), https://doi.org/10.1021/acs.jpcc.7b06303.

[69] T. A. Halgren and W. Damm, Curr. Opin. Struct. Biol. **11**, 236 (2001).